Available online at www.sciencedirect.com

ScienceDirect

Nuclear Physics A 982 (2019) 659–662

www.elsevier.com/locate/nuclphysa

Measurements of open charm production in Au+Au collisions at $\sqrt{s_{\rm NN}}$ = 200 GeV with the STAR experiment at RHIC

Sooraj Radhakrishnan for the STAR Collaboration

Lawrence Berkeley National Laboratory, Berkeley, CA 94720, USA

Abstract

We report in these proceedings on the measurements of collision centrality and transverse momentum ($p_{\rm T}$) dependences of the $\Lambda_c^{\pm}$ production in Au+Au collisions at $\sqrt{s_{\rm NN}}$ = 200 GeV, using the STAR Heavy Flavor Tracker (HFT). The $\Lambda_c^{\pm}$ signal significance is greatly improved with the addition of the high-statistics data set collected in 2016 and the use of a supervised machine learning method for topological reconstruction of the decay vertices. The measured $\Lambda_c^{\pm}/D^0$ ratio shows a significant enhancement compared to the PYTHIA prediction for p+p collisions, across the measured $p_{\rm T}$ range. We also report on the updated measurements of D^0 nuclear modification factors $R_{\rm AA}$ and $R_{\rm CP}$ using the 2014 data with the HFT. The measured D^0 $R_{\rm AA}$ in central collisions is lower than unity across the $p_{\rm T}$ interval of the measurement. The D^0 yields show strong suppression at high $p_{\rm T}$ (> 6 GeV/c) in central collisions, consistent with that of light flavor hadrons. The $c\bar{c}$ production cross section per binary nucleon collision at midrapidity in Au+Au collisions at 200 GeV is extracted based on the various charm hadron measurements by STAR. It is observed that while the charm hadrochemistry is significantly modified in Au+Au collisions compared to p+p collisions, the $c\bar{c}$ production cross section at midrapidity remains consistent between Au+Au and p+p collisions.

Keywords: Quark-gluon plasma, charm quark production, charm quark hadronization, heavy flavor energy loss

1. Introduction

Relativistic heavy-ion collisions at RHIC and LHC create a hot dense medium consisting of deconfined quarks and gluons, usually referred to as the Quark Gluon Plasma (QGP) [1]. In these collisions, heavy flavor quarks (charm and bottom) are predominantly produced through initial hard partonic scatterings and therefore are valuable probes to study the properties of the QGP [2, 3]. The measurements of charm hadron nuclear modification factor $R_{\rm AA}$ ($R_{\rm CP}$), ratio of charm hadron spectra in heavy-ion collisions to that in p+p (peripheral heavy-ion) collisions scaled by the number of binary collisions ($N_{\rm coll}$), provide insights into the energy loss mechanism of charm quarks in the QGP medium and help constrain model parameters [3, 4]. The hadronization of charm quarks in the presence of QGP can be studied through the measurement of yield ratios of charm hadrons, particularly the $\Lambda_c^{\pm}/D^0$ (D^0 here includes both D^0 and $\overline{D^0}$) yield ratio. An enhancement of this ratio, relative to that in p+p collisions, is expected in the intermediate $p_{\rm T}$ region (2 - 6 GeV/c) if charm quarks hadronize via the coalescence mechanism in the QGP [5, 6]. The magnitude of this enhancement is sensitive to the charm quark dynamics and the presence of diquarks in the medium [6, 7].

In these proceedings we present measurements of the $\Lambda_c^{\pm}/D^0$ yield ratio and the D^0 $R_{\rm AA}$ and $R_{\rm CP}$ in $\sqrt{s_{\rm NN}}$ = 200 GeV Au+Au collisions at RHIC, using the STAR Heavy Flavor Tracker (HFT). The $\Lambda_c^{\pm}/D^0$

https://doi.org/10.1016/j.nuclphysa.2018.10.050

yield ratio is measured as a function of p_T and centrality and is compared to model calculations. The D^0 R_{AA} and R_{CP} are presented for various centrality classes as a function of p_T and compared to similar measurements for light flavor hadrons as well as model calculations. The $c\bar{c}$ production cross section per binary nucleon collision at midrapidity in Au+Au collisions at $\sqrt{s_{NN}}$ = 200 GeV is also calculated using the extensive charm hadron yield measurements by STAR.

2. Experiment and Analysis

The STAR detector at RHIC has a full azimuthal acceptance and a pseudorapidity (η) coverage of $|\eta| < 1$ [8]. The Heavy Flavor Tracker [9] is a high-resolution silicon detector installed close to the beam pipe and provides an excellent track pointing resolution, e.g. less than 40 μm for kaons with p_T = 1 GeV/c. This allows to apply selections on the displaced decay vertex topology of heavy flavor hadrons, which greatly enhances the signal significance. Particle identification (PID) at STAR is provided by the ionization energy loss (dE/dx) measured in the Time Projection Chamber (TPC) and the velocity measured using the Time of Flight (TOF) detector [8]. About 900 M minimum-bias Au+Au events from the 2014 run and ∼1000 M minimum-bias Au+Au events from the 2016 run at RHIC are used.

The $\Lambda_c^\pm$ candidates are reconstructed via the $\Lambda_c^\pm \to p^\pm K^\mp \pi^\pm$ channel, using both 2014 and 2016 datasets. The supervised learning algorithm, Boosted Decision Trees (BDT), from the Toolkit for Multivariate Analysis (TMVA) [10] is used for signal and background separation. The BDT is trained using a signal sample of $\Lambda_c^\pm \to p^\pm K^\mp \pi^\pm$ decays simulated using PYTHIA [11], with detector effects taken into account, and a background sample from wrong-sign $pK\pi$ triplets from data. The use of BDT along with the combined 2014+2016 data gives a factor of 2 improvement in the $\Lambda_c^\pm$ signal significance compared to previous measurement [12]. The D^0 measurements are carried out using the 2014 data. The D^0 and $\overline{D^0}$ candidates are reconstructed through the $K^\mp \pi^\pm$ decay channel. Rectangular cuts on variables characterizing the decay topology, also optimized using TMVA, are used for signal and background separation. A measurement of the $D^\pm$ spectra, used in the $c\bar{c}$ production cross section estimation, is carried out using the 2016 data, with candidates reconstructed using the $D^\pm \to K^\mp \pi^\pm \pi^\pm$ channel. The TPC track reconstruction efficiency, acceptance corrections, and PID efficiency are evaluated using embedding and data-driven methods [13]. The HFT track matching and topological cut efficiencies are evaluated through a data-driven fast simulation which takes the HFT-to-TPC track matching ratios and track pointing resolutions from data as inputs. Additionally, a vertex resolution correction, which is more relevant for peripheral collisions, is applied to account for the contribution of the primary vertex resolution to the track pointing resolution in data.

3. Results

The left panel of Fig. 1 shows the $\Lambda_c^\pm/D^0$ ratio as a function of p_T for the 10-80% centrality class. The data shows a significant enhancement of the ratio compared to the PYTHIA prediction for p+p collisions. The SHM model [14] also underpredicts the data. The Ko model (for 0-5% centrality class) [6] and the Greco model (0-20%) [5] calculations include coalescence of thermalized charm quarks and are closer to the measured values. The right panel of Fig. 1 shows the $\Lambda_c^\pm/D^0$ ratio as a function of centrality (expressed in N_{part}). The $\Lambda_c^\pm/D^0$ ratio shows an increasing trend towards more central collisions. The measured value in the peripheral collisions is consistent with the value from p+p collisions at 7 TeV measured by ALICE [15].

The D^0 R_{AA}, measured down to zero p_T using the HFT data from 2014, is shown in the left panels of Fig. 2 for three centrality classes. The values at low p_T (< 2 GeV/c) differ from the previously published R_{AA} values from STAR using the 2010 and 2011 data [4]. The difference is due to an incorrect efficiency correction applied in the 2010/2011 analysis, and the corrected results are published in an erratum [16]. The figures also show the re-analyzed 2010/2011 results, which are consistent with the results from the HFT analysis of 2014 data. The D^0 R_{AA} values are below 1 at all p_T in central collisions. The R_{AA} values for p_T > 5 GeV/c show significant suppression in central collisions, and the suppression decreases towards more peripheral collisions, as the system size decreases. The right panels of Fig. 2 show the D^0 R_{CP}, relative to the 40-60% centrality class. The R_{CP} values are consistent with unity for p_T < 2 GeV/c, but decrease towards high p_T (> 6 GeV). The figure also shows the R_{CP} values for different light flavor hadrons in 200 GeV Au+Au collisions [17]. The R_{CP} values of D^0 show similar levels of suppression as light flavor hadrons

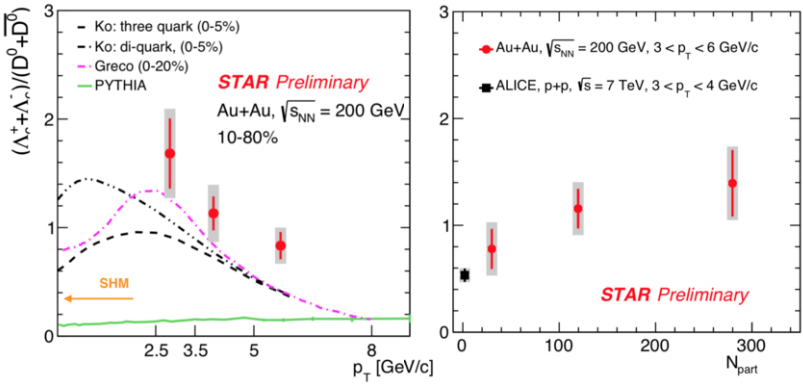

Fig. 1. The $\Lambda_c^{\pm}/D^0$ ratio as a function of p_T for 10-80% centrality class (left) and as a function of N_{part} for $3 < p_T < 6$ GeV/c (right), in Au+Au collisions at $\sqrt{s_{NN}} = 200$ GeV. The error bars and gray bands represent statistical and systematic uncertainties, respectively.

for $p_T > 5$ GeV/c. Comparisons to two model calculations which incorporate both collisional and medium-induced radiative energy loss for charm quarks are also shown in the figure. The Duke model [18] uses a modified Langevin equation to describe the charm quark transport in the medium and radiative energy loss, while the LBT [3] model uses a linearized Boltzman transport model with the higher-twist formalism for medium-induced radiative energy loss. Both models can well describe the data. The model parameters had been tuned to describe the previous STAR measurements from [4], and the new high precision results reported here can help better constrain the model parameters.

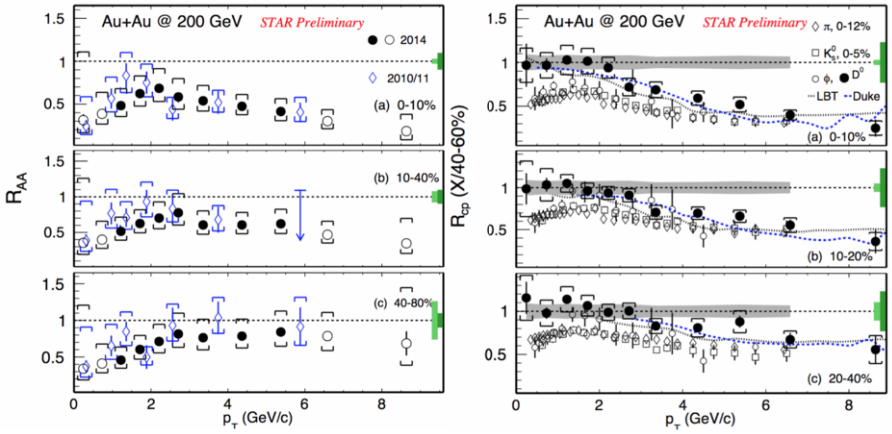

Fig. 2. The D^0 R_{AA} (left) and R_{CP} values relative to 40-60% centrality class (right) as a function of p_T for different centrality intervals. The solid circles in the left panels indicate that measured p+p yields are used for calculating R_{AA} and the open circles indicate that the p+p yields from an extrapolation using a Levy fit to the measured yields are used. The open diamonds are the values from reanalyzed 2010/2011 data. The error bars and brackets on the data points indicate statistical and systematic uncertainties respectively. The dark and light green boxes on the right of each panel show the global uncertainty from the reference (p+p cross section uncertainty for R_{AA} and N_{coll} uncertainty for 40-60% centrality for R_{CP}) and the N_{coll} uncertainty for the given centrality class, respectively. The shaded gray bands around 1 on the R_{CP} plots indicate the uncertainty from vertex resolution correction for the 40-60% centrality class.

In addition to the measurements of $\Lambda_c^{\pm}$ and D^0 production, STAR has also measured the $D_s^{\pm}$ [19] and $D^{\pm}$ yields [21] in 200 GeV Au+Au collisions. From these charm hadron yield measurements, we have extracted the $c\bar{c}$ production cross section per binary nucleon collision at midrapidity ($d\sigma^{c\bar{c}}/dy|_{y=0}$) in 200 GeV Au+Au collisions. The D^0 yield is measured down to zero p_T, while for the other charm hadron species, an extrapolation to zero p_T is used to calculate the total yield. The $D^{\pm}$ and $D_s^{\pm}$ spectra are extrapolated to zero p_T using Levy function fits. Fits using a power law function are used to estimate the systematic uncertainties

from fitting. For $\Lambda_c^{\pm}$, the three model calculations shown in Fig. 1 are used to extrapolate down to zero p_T. The mean value from the three fits is taken as the yield and the difference as systematics. For p+p collisions, the extrapolation of measured data [20] to zero p_T is carried out using a Levy function fit, while a fit using a power-law function is used to estimate the systematic uncertainty. The results are summarized in Table 1. The $c\bar{c}$ production cross section per binary nucleon collision at midrapidity measured in Au+Au collisions is consistent with that in p+p collisions within uncertainties. However, the D^0 and $D^{\pm}$ yields are suppressed, while those of $\Lambda_c^{\pm}$ and $D_s^{\pm}$ are enhanced, suggesting significant modifications to charm quark hadronization and hadrochemistry in the presence of the QGP medium.

	Charm hadron	Cross Section (μb)
Au+Au, 10-40%	D^0	41 ± 1 (stat) ± 5 (sys)
	$D^{\pm}$	18 ± 1 (stat) ± 3 (sys)
	$D_s^{\pm}$	15 ± 1 (stat) ± 5 (sys)
	$\Lambda_c^{\pm}$	78 ± 13 (stat) ± 28 (sys)
	$c\bar{c}$	152 ± 13 (stat) ± 29 (sys)
p+p	$c\bar{c}$	130 ± 30 (stat) ± 26 (sys)

Table 1. The charm hadron and $c\bar{c}$ production cross sections per binary nucleon collision at midrapidity in Au+Au and p+p collisions at $\sqrt{s_{NN}}$ = 200 GeV.

4. Summary

We have presented the measurements of the $\Lambda_c^{\pm}/D^0$ ratio as a function of collision centrality and p_T in Au+Au collisions at $\sqrt{s_{NN}}$ = 200 GeV. The ratio shows a significant enhancement compared to the values from PYTHIA for p+p collisions and also to SHM calculations. Model calculations with hadronization via coalescence are closer to the experimental measurements, suggesting that the coalescence mechanism plays an important role in charm quark hadronization in the QGP. The measurements of the D^0 R_{AA} and D^0 R_{CP} are also presented for 200 GeV Au+Au collisions. The R_{AA} and R_{CP} values show a strong suppression at high p_T in central collisions and the suppression decreases towards peripheral collisions. The R_{CP} values at high p_T (> 6 GeV/c) are consistent with those of light flavor hadrons, while they are larger for $p_T < 4$ GeV/c. Transport models with collisional and radiative energy losses are able to describe the measured R_{CP} values. The $c\bar{c}$ production cross section per binary nucleon collision at midrapidity in 200 GeV Au+Au collisions is also extracted from the measurements of D^0, $D^{\pm}$, $D_s^{\pm}$, $\Lambda_c^{\pm}$ yields by STAR, and is consistent with that in p+p collisions.

References

[1] B. Muller, J. Schukraft, and B. Wyslouch, Ann. Rev. Nucl. Part. Sci. **62**, 361 (2012).
[2] M. Cacciari *et al.*, Phys. Rev. Lett **95**, 122001 (2005).
[3] S. Cao *et al.*, Phys. Rev. C **94**, 014909 (2016).
[4] STAR Collaboraion, Phys. Rev. Lett. **113**, 142301, (2014).
[5] S. Ghosh, S. K. Das, V. Greco, S. Sarkar and J. E. Alam, Phys. Rev. D**90(5)**, 2-7 (2014).
[6] S. H. Lee, K. Ohnishi, S. Yasui, I.-K. Yoo and C. M. Ko Phys. Rev. Lett.**100**, 222301 (2008).
[7] Y. Oh, C. M. Ko, S. H. Lee and S. Yasui, Phys. Rev. C**79**, 044905 (2009).
[8] STAR Collaboration, Nucl. Inst. Meth. A**499**, 624632 (2003).
[9] G. Contin *et al.*, Nucl. Inst. Meth. A (in press), https://doi.org/10.1016/j.nima.2018.03.003.
[10] A. Hoecker *et al.* CERN-OPEN-2007-007
[11] T. Sjostrand, S. Mrenna and P. Skands, Journal of High Energy Physics**2006**, 026 (2006).
[12] G. Xie (STAR Collaboration), Nucl. Phys. A **967**, 928-931, 2017.
[13] STAR Collaboration, Phys. Rev. Lett.**113**, 142301 (2014).
[14] I. Kuznetsova and J. Rafelski, The European Physical Journal C**51** 113133 (2007).
[15] ALICE Collaboration, arXiv:1712.09581
[16] STAR Collaboration, arXiv:1809.08737
[17] STAR Collaboration, Phys. Rev. Lett. **97**, 152301 (2006); Phys. Rev. C **79**, 064903 (2009); Phys. Rev. Lett. **108**, 072301
[18] Y. Xu *et al.* Phys. Rev. C. **97**, 014907 (2018).
[19] L. Zhou (STAR Collaboration) Nucl. Phys. A. **967**, 620-623 (2017).
[20] STAR Collaboration Phys. Rev. D. **86**, 072013 (2012).
[21] J. Vanek (STAR Collaboration) Quark Matter 2018 Poster https://indico.cern.ch/event/656452/contributions/2859701/